Advances in Mathematical Physics

WILEY

RESEARCH ARTICLE OPEN ACCESS

Hopf Bifurcation Analysis and Matched Asymptotics for a Bi-Stable Flame Propagation Model

Saqib Zia[1] | Saeed ur Rahman[2] | José Luis Díaz Palencia[3] | Ghania Zia[2] | Wei Sin Koh[4] | Sultan Hussain[5]

[1]Department of Mathematics, COMSATS University Islamabad, Park Road Chak Shehzad, Islamabad, Pakistan | [2]Department of Mathematics, COMSATS University Islamabad, Abbottabad Campus, Abbottabad 22060, Pakistan | [3]Department of Mathematics and Education, Universidad a Distancia de Madrid, Via de Servicio A-6, 15, Madrid 28400, Spain | [4]Persiaran Perdana BBN Putra Nilai, INTI International University, Nilai 71800, Nergeri Sembilan, Malaysia | [5]Department of Mathematics and Statistics, College of Sciences, Imam Mohammad Ibn Saud Islamic University (IMSIU), Riyadh 11623, Saudi Arabia

Correspondence: Saeed ur Rahman (saeed@cuiatd.edu.pk)

Received: 27 October 2025 | **Revised:** 3 June 2026 | **Accepted:** 4 August 2026

Academic Editor: Igor Freire

Keywords: energy efficiency | geometric perturbation theory | Hopf bifurcation analysis | matched asymptotics

ABSTRACT

In this article, we consider a model for flame propagation dynamics influenced by both temperature and pressure. The model is based on nonlinear diffusion and incorporates elements from porous structure theory within the framework of partial differential equations. Initially, Hopf bifurcation analysis is used to identify equilibrium points where the system exhibits asymptotic stability. Subsequently, the solution profiles are derived using a combination of traveling wave solutions and geometric perturbation theory. The existence of finite propagation speed is demonstrated, and conditions for the stability of the system are established. Furthermore, through the method of matched asymptotic expansions, the inner (short-time) and outer (long-time or large-distance) solutions are connected, ensuring consistency in the asymptotic behavior across both regimes via Van Dyke's matching principle. Numerical simulations are also used to validate the results.

1 | Introduction

In various fields such as climate change, combustion, chemical kinetics, biology, and transport processes, the chemical and physical investigation in porous media plays a significant role (details for climate change and combustion are provided in [1–3], respectively).

The study of flame propagation in porous media has been a subject of great interest from both practical and theoretical perspectives. The model of flame propagation in the current article is derived from a classical parabolic model, incorporating a nonlinear diffusion term. Mathematically, it is described as follows:

$$\frac{\partial w_1}{\partial t} = \frac{\partial^2 w_1^m}{\partial x^2} + G(w_1, w_2) \tag{1}$$

$$\frac{\partial w_2}{\partial t} = \varepsilon \frac{\partial^2 w_2^m}{\partial x^2} + G(w_1, w_2), \tag{2}$$

where w_1 and w_1 represent the physical variables for temperature and pressure (see [4]) as follows:

$$\begin{aligned} T(x,t) &= hw_1(x,t) + (1-h)w_2(x,t), P(x,t) \\ &= \frac{1}{1-\widehat{\varepsilon}}(w_1(x,t) - \widehat{\varepsilon} w_2(x,t)), \end{aligned}$$

where $\widehat{\varepsilon}$ is the relation between the thermal driven and pressure driven diffusivities. If $G(w_1, w_2) = (1-w_2)(hw_1 + (1-h)w_2)$ with $m=1$ and $h \in [0,1]$, then Equations (1) and (2) represent a model in combustion theory. Fisher [5] was one of the first researchers to obtain useful results for this combustion model in the cases $h=0$ and $h=1$. Later, Billingham and Needham

[6] extended these results while working on genetic interactions in population dynamics. A few years later, Kolmogorov et al. [7] considered only Equation (2) with $h = 0$ and $m = 1$, obtaining the existence of solutions. The results for traveling waves analysis under the assumption $h = 0$ and $m = 1$ are obtained by Weinberger [8].

Shchelkin [9] studied the flow of gases in a tube geometry and used traveling wave analysis to obtain solutions. Brailovsky et al. [10] studied high hydraulic resistance in porous media and obtained exact solutions. In [4] and [11], Gordon introduced new variables, such as the concentration, pressure, and temperature of the deficient reactant, and obtained useful results for the system Equations (1) and (2) with $m = 1$. Later, Ghazaryan and Gordon [12] obtained exact solutions using a linear transformation between temperature and pressure variables.

If $G(w_1, w_2) = (1 - w_2)(w_2 - \mu_1)(hw_1 + (1 - h)w_2)$, where $h \in [0, 1]$ and $\mu_1 \in [0, 1]$, this type of nonlinearity is called bi-stable. This nonlinearity was used by Aronson and Weinberger [13]. Kanel [14] considered a one-dimensional bi-stable reaction case with $m = 1$ and used traveling wave theory to prove the existence of a solution with positive wave speed. Roussier [15] studied bi-stable nonlinearity with $w_2 = w_1$ and obtained the asymptotic behavior of the solution for Equation (1). Recently, Rahman and Palencia [16] used the p-Laplacian operator instead of the Gaussian diffusion operator and obtained analytical and computational results.

If $m = 1$ then the diffusion term is linear and the system (1) and (2) have many applications. For example, in the spatiotemporal SI model (Chen et. al [17]) and the zooplankton-phytoplankton model (Chen and Tian [18]). The main difference between the model in this article and previous models is the introduction of a nonlinear diffusion term instead of a linear one. The idea of introducing nonlinear diffusion was proposed in [19], where the author suggested different types of diffusion for various biological applications. In that work, nonlinear diffusion was used in a flame propagation model, and analytical solutions were obtained. The purpose of using the nonlinear diffusion term here is to study its effect on the model. Several scientists have worked in this direction, including [20–22].

Therefore, taking into account the bi-stable nonlinearity, let us consider Equations (1) and (2):

$$\begin{aligned} \frac{\partial w_1}{\partial t} &= \frac{\partial^2 w_1^m}{\partial x^2} + (1 - w_2)(w_2 - \mu_1)(hw_1 + (1 - h)w_2), \\ \frac{\partial w_2}{\partial t} &= \varepsilon \frac{\partial^2 w_2^m}{\partial x^2} + (1 - w_2)(w_2 - \mu_1)(hw_1 + (1 - h)w_2), \end{aligned} \tag{3}$$

where $h \in (0, 1), x \in \mathbb{R}, \mu_1 \in (0, 1), w_1(x, 0) = w_{1_0}(x) > 0$, and $w_2(x, 0) = w_{2_0}(x) > 0$, with $m > 1$ belongs to integer, $\varepsilon \in (0, 1)$, and $(w_{1_0}(x), w_{2_0}(x)) \in L^1(\mathbb{R}) \cap L^\infty(\mathbb{R})$.

The present study contributes to the expanding literature on nonlinear diffusion flame models by incorporating porous-medium-type nonlinear diffusion into a coupled reaction-diffusion framework. In comparison to classical flame models with linear diffusion, the nonlinear diffusion exponent significantly affects the bifurcation thresholds, stability properties, and dynamical behavior of the system. The proposed model shares important features with porous medium and p-Laplacian diffusion equations, both of which describe diffusion processes whose intensity depends on the state variable. The present work emphasizes that with the increase of nonlinear diffusion exponent m, the solution converges slowly and plays an active role in shaping oscillatory flame dynamics.

The objective of Section 2 is to perform a Hopf bifurcation analysis of the model (3). The approach follows Guo et al. [23], and we obtain equilibrium points where the solution of the system is asymptotically stable. Chen with other authors in [24–28], also used the Hopf bifurcation analysis and obtain the existence and stability for the solutions of predator–prey models. In Section 3, we use the traveling wave approach to convert the system of ordinary differential equations and then use the condition in which the solutions of the system converge. In Section 4, we use the geometric perturbation theory to perturb the problem. In Section 5, we obtain the analytical solution for perturbed the problem which is given in Section 4. In Section 6, we develop the numerical solution perturbed by the problem to validate our results. In Section 7, we obtain the unsteady solution close to the steady solution. In Section 8, we use the matched asymptotic expansions to connect the inner and outer solutions. The unpublished work by Rahman et al. [29] is available at SSRN.

2 | Hopf Bifurcation Analysis

In this section, we depart from the work by Guo et al. [23]. The idea is to find the equilibrium points where the asymptotic solutions are stable.

It is easily checked that for $(n_1, n_2, n_3) \in R$ and $\mu_1 \in (0, 1)$ then $(n_1, 1)$, (n_2, μ_1) and $(-\frac{(1-h)n_3}{h}, n_3)$, are the equilibrium points for the system (3) and we constrain the problem to the spatial domain $\Omega = (0, l\pi)$. Also, it is a well-known result that given the operator $w_1 \to -\frac{\partial^2 w_1}{\partial x^2}$ with w_1 being null at the boundary, the corresponding eigenvalue problem is as follows:

$$\phi'' + k\phi = 0 \quad \text{with} \quad \phi(0) = \phi(l\pi) = 0 \tag{4}$$

which has the set of eigenvalues $k_n = \frac{n^2}{l^2}$ $(n = 0, 1, 2, \ldots)$ and eigenfunctions $\phi_n = \sin \frac{n}{l} x$, for $n = 0, 1, 2, \ldots$ The system (3) is linearized at the equilibrium point $(-\frac{(1-h)n_3}{h}, n_3)$ and leads to:

$$\begin{pmatrix} \frac{\partial w_1}{\partial t} \\ \frac{\partial w_2}{\partial t} \end{pmatrix} = L \begin{pmatrix} w_1 \\ w_2 \end{pmatrix} := D \begin{pmatrix} \frac{\partial^2 w_1}{\partial x^2} \\ \frac{\partial^2 w_2}{\partial x^2} \end{pmatrix} + \begin{pmatrix} h(1 - n_3)(n_3 - \mu_1) & (1 - h)(1 - n_3)(n_3 - \mu_1) \\ h(1 - n_3)(n_3 - \mu_1) & (1 - h)(1 - n_3)(n_3 - \mu_1) \end{pmatrix} \begin{pmatrix} w_1 \\ w_2 \end{pmatrix}, \tag{5}$$

where $D = \mathrm{diag}(m(\frac{(h-1)n_3}{h})^{m-1}, m(n_3)^{m-1})$ is the diffusion matrix. Consider the characteristic equation $L(\phi, \psi) = \lambda(\phi, \psi)$ and let $(\phi, \psi) = \Sigma_{n=0}^{\infty}(a_n, b_n)\sin \frac{n}{l} x$, then we can find $\Sigma_{n=0}^{\infty}(J_n - \lambda I)(a_n,\ b_n)^T \sin \frac{n}{l} x = 0$, where

$$J_n := J - \left(\frac{n}{l}\right)^2 D = \begin{pmatrix} h(1-n_3)(n_3-\mu_1) - m\left(\frac{n}{l}\right)^2 \left(\frac{(h-1)n_3}{h}\right)^{m-1} & (1-h)(1-n_3)(n_3-\mu_1) \\ h(1-n_3)(n_3-\mu_1) & (1-h)(1-n_3)(n_3-\mu_1) - m\left(\frac{n}{l}\right)^2 (n_3)^{m-1} \end{pmatrix}, \quad (6)$$

for the characteristic equation, by taking $|J_n - \lambda I| = 0$, we obtain:

$$\lambda^2 - T_n\lambda + D_n = 0, \quad (7)$$

where

$$T_n = (1-n_3)(n_3-\mu_1) - \frac{mn^2 n_3^{m-1}}{l^2}\left[\left(\frac{h-1}{h}\right)^{m-1} + 1\right], \quad (8)$$

and

$$D_n = \frac{m^2 n^4 n_3^{2m-2}}{l^4}\left(\frac{h-1}{h}\right)^{m-1} - \frac{mn^2 n_3^{m-1}}{l^2}(1-n_3)(n_3-\mu_1)\left[h + \frac{(h-1)^m}{h^{m-1}}\right]. \quad (9)$$

When $n \ll l$ and $n_3 \in (-\infty, \mu_1] \cup (1, \infty)$, we have $T_n < 0$ and $D_n > 0$.

Now, define $\zeta_n(\lambda) = \lambda^2 - T_n\lambda + D_n$. For $n \geq 0$, the above conditions imply that $T_n < 0$ and $D_n > 0$. Therefore, for any $n \geq 0$, the roots $\zeta_{1,n}$ and $\zeta_{2,n}$ of the equation $\zeta_n(\lambda) = 0$ are negative.

Next, we need to show that there exists $\delta > 0$, which is independent of n, such that $\zeta_{1,n} \leq -\delta$ and $\zeta_{2,n} \leq -\delta$. Suppose $\lambda = n^2\lambda$, then we have

$$\zeta_n(\lambda) = n^4\lambda^2 - n^2 T_n\lambda + D_n = \psi_n(\zeta).$$

After solving, we get:

$$\lim_{n\to\infty} \frac{\psi_n(\zeta)}{n^4} = \zeta^2 + \frac{mn_3^{m-1}}{l^2}\left[\left(\frac{h-1}{h}\right)^{m-1} + 1\right]\zeta + \frac{m^2 n_3^{2m-2}}{l^4}\left(\frac{h-1}{h}\right)^{m-1}. \quad (10)$$

This equation shows that for large n, the roots of $\psi_n(\zeta)$ are negative. Therefore, we can choose δ such that $\zeta_{1,n} \leq -\delta$ and $\zeta_{2,n} \leq -\delta$, which implies that the system (3) is asymptotically stable at the equilibrium point $\left(-\frac{(1-h)n_3}{h}, n_3\right)$. For the equilibrium point $(n_1, 1)$, the linearized form of system (3) is as follows:

$$\begin{pmatrix} \frac{\partial w_1}{\partial t} \\ \frac{\partial w_2}{\partial t} \end{pmatrix} = L\begin{pmatrix} w_1 \\ w_2 \end{pmatrix} := D\begin{pmatrix} \frac{\partial^2 w_1}{\partial x^2} \\ \frac{\partial^2 w_2}{\partial x^2} \end{pmatrix} + \begin{pmatrix} 0 & -(1-\mu_1)(hn_1+1-h) \\ 0 & -(1-\mu_1)(hn_1+1-h) \end{pmatrix}\begin{pmatrix} w_1 \\ w_2 \end{pmatrix}, \quad (11)$$

where $D = \mathrm{diag}(mn_1^{m-1}, m)$ is the diffusion matrix. Consider the characteristic equation $L(\phi, \psi) = \lambda(\phi, \psi)$. Let $(\phi, \psi) = \sum_{n=0}^{\infty}(a_n, b_n)\sin\frac{n}{l}x$. Then we can find:

$$\sum_{n=0}^{\infty}(J_n - \lambda I)(a_n, b_n)^T \sin\frac{n}{l}x = 0,$$

where

$$J_n := J - \left(\frac{n}{l}\right)^2 D = \begin{pmatrix} -\left(\frac{n}{l}\right)^2 mn_1^{m-1} & -(1-\mu_1)(hn_1+1-h) \\ 0 & -(1-\mu_1)(hn_1+1-h) - \left(\frac{n}{l}\right)^2 m \end{pmatrix}. \quad (12)$$

For the characteristic equation, we take $|J_n - \lambda I| = 0$, giving:

$$\lambda^2 + T_n\lambda + D_n = 0, \quad (13)$$

where

$$T_n = (1-\mu_1)(hn_1+1-h) + \frac{n^2 m}{l^2} + \frac{n^2 mn_1^{m-1}}{l^2}, \quad (14)$$

and

$$D_n = \frac{n^2 m}{l^2}(1-\mu_1)(hn_1+1-h) + \frac{n^4 m^2 n_1^{m-1}}{l^4}. \quad (15)$$

If $n_1 \geq 0$, then $T_n > 0$ and $D_n > 0$.

Now, suppose $\zeta_n(\lambda) = \lambda^2 + T_n\lambda + D_n$, and for $n \geq 0$, $n_1 \geq 0$, we have $T_n > 0$ and $D_n > 0$. Therefore, for any $n \geq 0$ and $\zeta_n(\lambda) = 0$, the roots $\zeta_{1,n}$ and $\zeta_{2,n}$ are negative.

Next, we need to show that there exists $\delta > 0$, independent of n, such that $\zeta_{1,n} \leq -\delta$ and $\zeta_{2,n} \leq -\delta$. Suppose $\lambda = n^2\lambda$, then:

$$\zeta_n(\lambda) = n^4\lambda^2 - n^2 T_n\lambda + D_n = \psi_n(\zeta).$$

After solving, we get:

$$\lim_{n\to\infty} \frac{\psi_n(\zeta)}{n^4} = \zeta^2 + \left(\frac{m}{l^2} + \frac{mn_1^{m-1}}{l^2}\right)\zeta + \frac{m^2 n_1^{2m-2}}{l^4}. \quad (16)$$

This equation shows that for large n, the roots of $\psi_n(\zeta)$ are negative. Therefore, we can choose δ such that $\zeta_{1,n} \leq -\delta$ and $\zeta_{2,n} \leq -\delta$, which shows that the system (3) is asymptotically stable at the equilibrium point $(n_1, 1)$. For the equilibrium point (n_2, μ_1), the linearized form of system (3) is as follows:

$$\begin{pmatrix} \frac{\partial w_1}{\partial t} \\ \frac{\partial w_2}{\partial t} \end{pmatrix} = L\begin{pmatrix} w_1 \\ w_2 \end{pmatrix} :=D\begin{pmatrix} \frac{\partial^2 w_1}{\partial x^2} \\ \frac{\partial^2 w_2}{\partial x^2} \end{pmatrix} + \begin{pmatrix} 0 & (1-\mu_1)\left(\frac{hn_2}{\mu_1}+1-h\right) \\ 0 & (1-\mu_1)\left(\frac{hn_2}{\mu_1}+1-h\right) \end{pmatrix}\begin{pmatrix} w_1 \\ w_2 \end{pmatrix}, \tag{17}$$

where $D=\mathrm{diag}(mn_2^{m-1}, m\mu_1^{m-1})$ is the diffusion matrix.

Consider the characteristic equation $L(\phi,\psi)=\lambda(\phi,\psi)$. Let $(\phi,\psi)=\sum_{n=0}^{\infty}(a_n,b_n)\sin\frac{n}{l}x$. Then, we can find:

$$\sum_{n=0}^{\infty}(J_n-\lambda I)(a_n,b_n)^T\sin\frac{n}{l}x=0,$$

where

$$J_n:=J-\left(\frac{n}{l}\right)^2 D=\begin{pmatrix} -\left(\frac{n}{l}\right)^2 mn_2^{m-1} & (1-\mu_1)\left(\frac{hn_2}{\mu_1}+1-h\right) \\ 0 & (1-\mu_1)\left(\frac{hn_2}{\mu_1}+1-h\right)-\left(\frac{n}{l}\right)^2 m\mu_1^{m-1} \end{pmatrix}. \tag{18}$$

For the characteristic equation, taking $|J_n-\lambda I|=0$, we have:

$$\lambda^2-T_n\lambda+D_n=0, \tag{19}$$

where

$$T_n=(1-\mu_1)\left(\frac{hn_2}{\mu_1}+1-h\right)-\frac{n^2m\mu_1^{m-1}}{l^2}-\frac{n^2mn_2^{m-1}}{l^2}, \tag{20}$$

and

$$D_n=-\frac{n^2m}{l^2}(1-\mu_1)\left(\frac{hn_2}{\mu_1}+1-h\right)+\frac{n^4m^2n_2^{m-1}\mu_1^{m-1}}{l^4}. \tag{21}$$

If $n_2\le\mu_1-\frac{\mu_1}{h}+\frac{n^2m\mu_1^m}{hl^2(1-\mu_1)}$, then $T_n<0$ and $D_n>0$.

Assume $\beta_n(\lambda)=\lambda^2+T_n\lambda+D_n$, and for $n\ge 0$, $n_2\le\mu_1-\frac{\mu_1}{h}+\frac{n^2m\mu_1^m}{hl^2(1-\mu_1)}$, we have $T_n<0$ and $D_n>0$. Therefore, for any $n\ge 0$ and $\beta_n(\lambda)=0$, the roots $\beta_{1,n}$ and $\beta_{2,n}$ are negative.

Next, we need to show that there exists $\delta>0$, independent of n, such that $\beta_{1,n}\le-\delta$ and $\beta_{2,n}\le-\delta$. Suppose $\lambda=n^2\lambda$, then:

$$\beta_n(\lambda)=n^4\lambda^2-n^2T_n\lambda+D_n=\psi_n(\beta).$$

After solving, we get:

$$\lim_{n\to\infty}\frac{\psi_n(\beta)}{n^4}=\beta^2+\left(\frac{m\mu_1^{m-1}}{l^2}+\frac{mn_2^{m-1}}{l^2}\right)\beta+\frac{m^2n_2^{m-1}\mu_1^{m-1}}{l^4}. \tag{22}$$

This equation shows that for large n, the roots of $\psi_n(\beta)$ are negative. Therefore, we can choose δ such that $\beta_{1,n}\le-\delta$ and $\beta_{2,n}\le-\delta$, which shows that the system (3) is asymptotically stable at the equilibrium point (n_2,μ_1).

It is noted that the Hopf bifurcation mechanism results of model (3) are obtained by the interaction between the nonlinear reaction kinetics and the nonlinear porous-medium diffusion. The reaction term $((1-w_2)(w_2-\mu_1)(hw_1+(1-h)w_2))$ provides the nonlinear response which is responsible for disrupting the steady state and the cause of oscillatory dynamics. At the same time, the nonlinear diffusion exponent (m) occurs in the coefficients of the characteristic equation which affect both the trace and determinant of the linearized system. Consequently, the critical conditions for Hopf bifurcation depend not only on the reaction parameters but also on the strength of nonlinear diffusion. This illustrates that the start of periodic oscillations is governed by the coupling of nonlinear reaction and nonlinear diffusion effects. In comparison to classical reaction-diffusion models with linear diffusion, the present analysis reveals that the increase of m the solution converges slowly, which affects the stability properties and bifurcation thresholds.

3 | Traveling Waves Analysis

The purpose of this section is to employ traveling waves to derive the solution profiles for the system (3). To accomplish this, we assume that:

$$w_1(x,t)=G_4(\zeta),\ w_2(x,t)=G_5(\zeta),$$

where $\zeta=x-at\in\mathbb{R}$ and a represents the wave propagation speed. The functions:

$$G_4:\mathbb{R}\to(0,\infty),\ G_5:\mathbb{R}\to(0,\infty),$$

are bounded, that is, $G_4\in L^\infty(\mathbb{R}), G_5\in L^\infty(\mathbb{R})$. Substituting the traveling wave assumption into the system (3), we obtain:

$$-aG_4'=(G_4^m)''+(1-G_5)(G_5-\mu_1)(hG_4+(1-h)G_5), \tag{23}$$

$$-aG_5'=(G_5^m)''+(1-G_5)(G_5-\mu_1)(hG_4+(1-h)G_5), \tag{24}$$

to investigate the solutions in the phase space, we define the following variables representing density and flux:

$$X_4=G_4(\zeta),\ Y_4=(G_4^m(\zeta))',\ X_5=G_5(\zeta),\ Y_5=(G_5^m(\zeta))'. \tag{25}$$

Substituting (25) into the system (23) and (24), we can rewrite the system as follows:

$$
\begin{aligned}
X_4' &= \frac{1}{m} X_4^{1-m} Y_4, \\
Y_4' &= \frac{-a}{m} X_4^{1-m} Y_4 - (1 - X_5)(X_5 - \mu_1)[hX_4 + (1-h)X_5], \\
X_5' &= \frac{1}{m} X_5^{1-m} Y_5, \\
Y_5' &= \frac{-a}{m} X_5^{1-m} Y_5 - (1 - X_5)(X_5 - \mu_1)[hX_4 + (1-h)X_5].
\end{aligned} \tag{26}
$$

The system (26) has critical points at $(n_1, 0, 1, 0)$, $(n_2, 0, \mu_1, 0)$, and $(\frac{-(1-h)n_3}{h}, 0, n_3, 0)$.

Theorem 1. *The traveling wave solution of the system (26) close to critical points $(n_1, 0, 1, 0)$, $(n_2, 0, \mu_1, 0)$ and $(\frac{-(1-h)n_3}{h}, 0, n_3, 0)$ are stable.*

Proof. For the point $(X_4, Y_4, X_5, Y_5) = (n_1, 0, 1, 0)$, we state the following lemma. □

Lemma 1. *The critical point $(n_1, 0, 1, 0)$ corresponds to a degenerate node with the following properties:*

- *For $h(1 - n_1) > 1$, there are three negative eigenvalues and one zero eigenvalue.*
- *For $h(1 - n_1) < 1$, there are one zero, one positive, and two negative eigenvalues.*

Moreover, close to critical point $(n_1, 0, 1, 0)$, the traveling wave solution of the system is stable.

Proof. Let us suppose that in proximity to the stationary condition:

$$\bar{X_4} = -X_4 + 1, \ X_4 << 1. \tag{27}$$

Under this assumption, the system (26) can be represented as follows in the vicinity of the stationary condition:

$$
\begin{pmatrix} X_3' \\ Y_3' \\ \bar{X_4}' \\ Y_4' \end{pmatrix} = \begin{pmatrix} 0 & \frac{1}{m}(n_1)^{1-m} & 0 & 0 \\ 0 & -\frac{a}{m}(n_1)^{1-m} & (\mu_1 - 1)(h(1-n_1) - 1) & 0 \\ 0 & 0 & 0 & \frac{1}{m} \\ 0 & 0 & (\mu_1 - 1)(h(1-n_1) - 1) & -\frac{a}{m} \end{pmatrix} \begin{pmatrix} X_3 \\ Y_3 \\ \bar{X_4} \\ Y_4 \end{pmatrix}. \tag{28}
$$

The eigenvalues of the system are given as follows:

$$
\begin{aligned}
&(\lambda_1', \lambda_2', \lambda_3', \lambda_4') = \\
&\left(0, -\frac{a}{m} n_1^{1-m}, -\frac{a}{2m} + \frac{1}{2}\sqrt{\frac{a^2}{m^2} - \frac{4(1-\mu_1)[h(1-n_1) - 1]}{m}}, \right. \\
&\left. -\frac{a}{2m} - \frac{1}{2}\sqrt{\frac{a^2}{m^2} - \frac{4(1-\mu_1)[h(1-n_1) - 1]}{m}} \right).
\end{aligned} \tag{29}
$$

The nonnegative eigenvalues exist if:

$$
\begin{aligned}
&a^2 - 4m(1-\mu_1)[h(1-n_1) - 1] \geq 0 \text{ and} \\
&(1-\mu_1)[h(1-n_1) - 1] \leq 0.
\end{aligned} \tag{30}
$$

The minimum wave speed $a_{\min}$ is given as follows:

$$a_{\min} = 2\sqrt{m(1-\mu_1)[h(1-n_1) - 1]}. \tag{31}$$

The minimum speed exists if $h(1 - n_1) > 1$. The corresponding exponential profiles are as follows:

$$
\begin{aligned}
&X_4 = E_3 e^{-\lambda_3' t}, \ E_3 > 0, \\
&\lambda_3' = -\frac{a}{2m} + \frac{1}{2}\sqrt{\frac{a^2}{m^2} - \frac{4(1-\mu_1)[h(1-n_1) - 1]}{m}},
\end{aligned} \tag{32}
$$

and

$$
\begin{aligned}
&X_5 = E_4 e^{-\lambda_4' t}, \ E_4 \in \mathbb{R}, \\
&\lambda_4' = -\frac{a}{2m} - \frac{1}{2}\sqrt{\frac{a^2}{m^2} - \frac{4(1-\mu_1)[h(1-n_1) - 1]}{m}}.
\end{aligned} \tag{33}
$$

These expressions indicate that the wave solutions converge to the critical point $(n_1, 0, 1, 0)$. □

Lemma 2. *The degenerate node is associated with the critical point $(n_2, 0, \mu_1, 0)$ and has the following properties:*

- *For $h(\mu_1 - n_2) > \mu_1$, there are three negative eigenvalues and one zero eigenvalue.*
- *For $h(\mu_1 - n_2) < \mu_1$, there are one zero, one positive, and two negative eigenvalues.*

Moreover, close to critical point $(n_2, 0, \mu_1, 0)$, the traveling wave solution of the system is stable.

Proof. Let us make the assumption that in proximity to the stationary condition:

$$\bar{X_4} = -\mu + X_4, \ X_4 << 1. \tag{34}$$

Under this assumption, the system (26) can be represented as follows in the vicinity of the stationary condition:

$$
\begin{pmatrix} X_3' \\ Y_3' \\ \bar{X_4}' \\ Y_4' \end{pmatrix} = \begin{pmatrix} 0 & \frac{1}{m}(n_2)^{1-m} & 0 & 0 \\ 0 & -\frac{a}{m}(n_2)^{1-m} & (\mu_1 - 1)(h(\mu_1 - n_2) - \mu_1) & 0 \\ 0 & 0 & 0 & \frac{1}{m}(\mu_1)^{1-m} \\ 0 & 0 & (\mu_1 - 1)(h(\mu_1 - n_2) - \mu_1) & -\frac{a}{m}(\mu_1)^{1-m} \end{pmatrix} \begin{pmatrix} X_3 \\ Y_3 \\ \bar{X_4} \\ Y_4 \end{pmatrix}. \tag{35}
$$

□

The corresponding eigenvalues are given as follows:

$$(\lambda_5', \lambda_6', \lambda_7', \lambda_8') = \Bigg(0, -\frac{an_2^{1-m}}{m}, -\frac{a\mu_1^{1-m}}{2m} + \frac{1}{2}\sqrt{\left(\frac{a\mu_1^{1-m}}{m}\right)^2 + \frac{4\mu_1^{1-m}(1-\mu_1)[\mu_1 - h(\mu_1 - n_2)]}{m}}, -\frac{a\mu_1^{1-m}}{2m} - \frac{1}{2}\sqrt{\left(\frac{a\mu_1^{1-m}}{m}\right)^2 + \frac{4\mu_1^{1-m}(1-\mu_1)[\mu_1 - h(\mu_1 - n_2)]}{m}}\Bigg). \tag{36}$$

The nonnegative eigenvalues exist if:

$$n_2 \le \frac{1}{h}\left[\mu_1(h-1) - \frac{a^2\mu_1^{1-m}}{4m(1-\mu_1)}\right] \text{ and } (1-\mu_1[\mu_1 - h(\mu_1 - n_2)] \ge 0. \tag{37}$$

The minimum wave speed $a_{\min}$ is as follows:

$$a_{\min} = 2\sqrt{m(1-\mu_1)[h(\mu_1 - n_2) - \mu_1]\mu_1^{m-1}}. \tag{38}$$

The minimum speed exists if $h(\mu_1 - n_2) > \mu_1$. The exponential profile of the solution is as follows:

$$X_4 = E_7 e^{-\lambda_7' t}, \ E_7 > 0, \ \lambda_7' = -\frac{a\mu_1^{1-m}}{2m} + \frac{1}{2}\sqrt{\left(\frac{a\mu_1^{1-m}}{m}\right)^2 + \frac{4\mu_1^{1-m}(1-\mu_1)[\mu_1 - h(\mu_1 - n_2)]}{m}}, \tag{39}$$

and

$$X_5 = E_8 e^{-\lambda_8' t}, \ E_8 \in \mathbb{R}, \ \lambda_8' = -\frac{a\mu_1^{1-m}}{2m} - \frac{1}{2}\sqrt{\left(\frac{a\mu_1^{1-m}}{m}\right)^2 + \frac{4\mu_1^{1-m}(1-\mu_1)[\mu_1 - h(\mu_1 - n_2)]}{m}}. \tag{40}$$

These expressions indicate that the wave solutions converge near the critical point $(n_2, 0, \mu_1, 0)$.

Lemma 3. *The degenerate node is associated with the critical point* $(\frac{-(1-h)n_3}{h}, 0, n_3, 0)$, *with the following properties:*

- *For* $(1-n_3)(n_3-\mu_1) < 0$, *there are three negative eigenvalues and one zero eigenvalue.*
- *For* $(1-n_3)(n_3-\mu_1) > 0$, *there are one zero, one positive, and two negative eigenvalues.*

Moreover, close to critical point $(\frac{-(1-h)n_3}{h}, 0, n_3, 0)$, *the traveling wave solution of the system is stable.*

Proof. Let us make the assumption that in the vicinity of the stationary condition:

$$\bar{X_4} = -X_4 + n_3, \ X_4 << 1. \tag{41}$$

Under this assumption, the system (26) can be represented as follows in its proximity to the stationary condition:

$$\begin{pmatrix} X_3' \\ Y_3' \\ \bar{X_4}' \\ Y_4' \end{pmatrix} = \begin{pmatrix} 0 & \frac{1}{m}\left(\frac{-(1-h)n_3}{h}\right)^{1-m} & 0 & 0 \\ 0 & -\frac{a}{m}\left(\frac{-(1-h)n_3}{h}\right)^{1-m} & (1-n_3)(n_3-\mu_1)(1-h) & 0 \\ 0 & 0 & 0 & \frac{1}{m}(n_3)^{1-m} \\ 0 & 0 & (1-n_3)(n_3-\mu)(1-h) & -\frac{a}{m}(n_3)^{1-m} \end{pmatrix} \begin{pmatrix} X_3 \\ Y_3 \\ \bar{X_4} \\ Y_4 \end{pmatrix}. \tag{42}$$

The corresponding eigenvalues are as follows:

$$(\lambda_9', \lambda_{10}', \lambda_{11}', \lambda_{12}') = \Bigg(0, -\frac{a}{m}\left(\frac{-(1-h)n_3}{h}\right)^{1-m}, -\frac{an_3^{1-m}}{2m} + \frac{1}{2}\sqrt{\left(\frac{an_3^{1-m}}{m}\right)^2 + \frac{4n_3^{1-m}(1-n_3)(n_3-\mu_1)(1-h)}{m}}, -\frac{an_3^{1-m}}{2m} - \frac{1}{2}\sqrt{\left(\frac{an_3^{1-m}}{m}\right)^2 + \frac{4n_3^{1-m}(1-n_3)(n_3-\mu_1)(1-h)}{m}}\Bigg). \tag{43}$$

The nonnegative eigenvalues are given as follows:

$$n_3 > \mu_1 \text{ and } 0 < n_3 < 1. \tag{44}$$

The minimum wave speed $a_{\min}$ is as follows:

$$a_{\min} = 2\sqrt{\frac{m(1-h)(1-n_3)(n_3-\mu_1)}{n_3^{1-m}}}. \tag{45}$$

The solution in exponential form is as follows:

$$X_4 = E_{11} e^{-\lambda_{11}' t}, \quad E_{11} > 0, \quad \lambda_{11}' = -\frac{an_3^{1-m}}{2m} + \frac{1}{2}\sqrt{\left(\frac{an_3^{1-m}}{m}\right)^2 + \frac{4n_3^{1-m}(1-n_3)(n_3-\mu_1)(1-h)}{m}}, \tag{46}$$

and

$$X_5 = E_{12} e^{-\lambda_{12}' t}, \quad E_{12} \in \mathbb{R}, \quad \lambda_{12}' = -\frac{a n_3^{1-m}}{2m} - \frac{1}{2}\sqrt{\left(\frac{a n_3^{1-m}}{m}\right)^2 + \frac{4 n_3^{1-m}(1-n_3)(n_3-\mu_1)(1-h)}{m}}. \tag{47}$$

These expressions show that the wave solutions converge near the critical point $(\frac{-(1-h)n_3}{h}, 0, n_3, 0)$. $\square$

4 | Geometric Perturbation Theory

The purpose of this section is to apply perturbation theory to develop a perturbed manifold near the critical points of the system (26). This technique helps us obtain traveling wave solutions. We begin by defining the manifold Ω_2, which is close to the critical point $(n_1, 0, 1, 0)$, as follows:

$$\Omega_2 = \left\{ X_4' = \frac{1}{m} {X_4}^{1-m} Y_4;\ Y_4' = \frac{-a}{m} {X_4}^{1-m} Y_4 \right\}. \tag{48}$$

The perturbed manifold close to Ω_2 is given as follows:

$$\Omega_{2,\varepsilon} = \left\{ \begin{array}{c} X_4 = n_1; \\ X_5 = 1-\varepsilon; \\ X_4' = \dfrac{1}{m} X_4^{1-m} Y_4; \\ Y_4' = \dfrac{-a}{m} X_4^{1-m} Y_4 - (1-\varepsilon-\mu_1)[h X_4 + (1-h)(1-\varepsilon)]\varepsilon \end{array} \right\}, \tag{49}$$

where ε is a small parameter. Similarly, we define the manifold Ω_3, which is close to the critical point $(n_1, 0, 1, 0)$, as follows:

$$\Omega_3 = \left\{ \begin{array}{l} X_5' = \dfrac{1}{m} X_5^{1-m} Y_5; \\ Y_5' = \dfrac{-a}{m} X_5^{1-m} Y_5 \end{array} \right\}. \tag{50}$$

The perturbed manifold close to Ω_3 is defined as follows:

$$\Omega_{3,\varepsilon} = \left\{ \begin{array}{c} X_4 = n_1; \\ X_5 = 1-\varepsilon; \\ X_5' = \dfrac{1}{m} X_5^{1-m} Y_5; \\ Y_5' = \dfrac{-a}{m} X_5^{1-m} Y_5 - (1-\varepsilon-\mu_1)[h n_1 + (1-h) X_5]\varepsilon \end{array} \right\}. \tag{51}$$

Next, we define the two-dimensional manifold Ω_4, which is close to the critical point $(n_2, 0, \mu_1, 0)$:

$$\Omega_4 = \left\{ \begin{array}{l} X_4' = \dfrac{1}{m} X_4^{1-m} Y_4; \\ Y_4' = \dfrac{-a}{m} X_4^{1-m} Y_4 \end{array} \right\}. \tag{52}$$

The perturbed manifold close to Ω_4 is given as follows:

$$\Omega_{4,\varepsilon} = \left\{ \begin{array}{c} X_4 = n_2; \\ X_5 = \mu_1 + \varepsilon; \\ X_4' = \dfrac{1}{m} X_4^{1-m} Y_4; \\ Y_4' = \dfrac{-a}{m} X_4^{1-m} Y_4 - (1-\mu_1-\varepsilon)[h X_4 + (1-h)(\mu_1+\varepsilon)]\varepsilon \end{array} \right\}. \tag{53}$$

We also define the manifold Ω_5 as follows:

$$\Omega_5 = \left\{ \begin{array}{l} X_5' = \dfrac{1}{m} X_5^{1-m} Y_5; \\ Y_5' = \dfrac{-a}{m} X_5^{1-m} Y_5 \end{array} \right\}. \tag{54}$$

The perturbed manifold $\Omega_{5,\varepsilon}$ is given as follows:

$$\Omega_{5,\varepsilon} = \left\{ \begin{array}{c} X_4 = n_2; \\ X_5 = \mu_1 + \varepsilon; \\ X_5' = \dfrac{1}{m} X_5^{1-m} Y_5; \\ Y_5' = \dfrac{-a}{m} X_5^{1-m} Y_5 - (1-\mu_1-\varepsilon)[h n_2 + (1-h) X_5]\varepsilon \end{array} \right\}. \tag{55}$$

Finally, close to the critical point $(\frac{-(1-h)n_3}{h}, 0, n_3, 0)$, we define the manifold Ω_6 as follows:

$$\Omega_6 = \left\{ \begin{array}{l} X_4' = \frac{1}{m} X_4^{1-m} Y_4; \\ Y_4' = \frac{-a}{m} X_4^{1-m} Y_4 \end{array} \right\}. \tag{56}$$

The perturbed manifold close to Ω_6 is given as follows:

$$\Omega_{6,\varepsilon} = \left\{ \begin{array}{c} X_4 = \frac{-(1-h)n_3}{h} + \varepsilon; \\ X_5 = n_3; \\ X_4' = \frac{1}{m} X_4^{1-m} Y_4; \\ Y_4' = \frac{-a}{m} X_4^{1-m} Y_4 - (1-n_3)(n_3-\mu_1)(hX_4 + (1-h)n_3) \end{array} \right\}. \tag{57}$$

Finally, the manifold Ω_7 is defined as follows:

$$\Omega_7 = \left\{ \begin{array}{l} X_5' = \frac{1}{m} X_5^{1-m} Y_5; \\ Y_5' = \frac{-a}{m} X_5^{1-m} Y_5 \end{array} \right\}. \tag{58}$$

The perturbed manifold close to Ω_7 is given as follows:

$$\Omega_{7,\varepsilon} = \left\{ \begin{array}{c} X_4 = \frac{-(1-h)n_3}{h} + \varepsilon; \\ X_5 = n_3; \\ X_5' = \frac{1}{m} X_5^{1-m} Y_5; \\ Y_5' = \frac{-a}{m} X_5^{1-m} Y_5 - h(1-n_3)(X_5-\mu_1)\varepsilon \end{array} \right\}. \tag{59}$$

From [14], the manifolds Ω_i, where $i = 2, 3, \ldots, 7$, satisfy the Fenichel invariant manifold theorem. Additionally, the newly defined perturbed manifolds $\Omega_{i,\varepsilon}$, where $i = 2, 3, \ldots, 7$, provide analytical profiles of the solutions. Furthermore, the distance between the manifolds Ω_i and $\Omega_{i,\varepsilon}$ for $i = 2, 3, \ldots, 7$ satisfies the normal hyperbolic condition. The profiles of traveling waves can be derived by using either the dimensionally reduced manifolds Ω_i, where $i = 2, 3, \ldots, 7$, or their asymptotic counterparts $\Omega_{i,\varepsilon}$.

5 | Traveling Wave Profiles and Finite Propagation

The perturbed manifold $\Omega_{2,\varepsilon}$, yields a set of trajectories in the phase plane (X_4, Y_4) by solving the following equation:

$$\begin{aligned} \frac{dY_4}{dX_4} &= -a + m[(1-\varepsilon-\mu_1)(hX_4 + (1-h)(1-\varepsilon))] \\ \varepsilon X_4^{m-1} \frac{1}{Y_4} &= H(a, X_4, X_5, Y_4). \end{aligned} \tag{60}$$

where $0 < X_4 < n_1$, $0 < X_5 < 1$, and $Y_4 > 0$. The above equation shows that for $a < 0$ then $\frac{dY_4}{dX_4} > 0$ and for increasing values of a then $\frac{dY_4}{dX_4} < 0$. Since $H(a, X_4, X_5, Y_4)$ is continuous, then there exists regular trajectory by solving the following equation

$$\begin{aligned} &-a - m[(1-\mu_1)(hX_4 + (1-h))] \\ &\varepsilon X_4^{m-1} \frac{1}{Y_4} = H(a, X_4, X_5, Y_4) = 0, \end{aligned}$$

where $\varepsilon^2 \to 0$. After using Equation (25), we have

$$-a(G_4^m)' - m[(1-\mu_1)(hG_4 + (1-h))]\varepsilon G_4^{m-1} = 0.$$

After solving the above equation, we have

$$G_4(x,t) = \frac{-(1-h)}{h} + \left(w_{10}(x) + \frac{(1-h)}{h} \right) e^{-\frac{\varepsilon h(1-\mu_1)\zeta}{am}},$$

which implies that

$$w_1(x,t) = \frac{-(1-h)}{h} + \left(w_{10}(x) + \frac{(1-h)}{h} \right) e^{-\frac{\varepsilon h(1-\mu_1)(x-at)}{a}}. \tag{61}$$

For the trajectories in the phase plane (X_5, Y_5), we consider perturbed manifold $(\Omega_{3,\varepsilon})$ and using the same procedure as that obtained for the trajectories for perturbed manifold $(\Omega_{2,\varepsilon})$ we have:

$$-aY_5 - \varepsilon m(1-\varepsilon-\mu_1)(hn_1 + (1-h)X_5)X_5^{m-1} = 0.$$

After using Equation (25), we have

$$-a(G_5^m)' - \varepsilon m(1-\varepsilon-\mu_1)(hn_1 + (1-h)G_5)G_5^{m-1} = 0,$$

where $\varepsilon^2 \to 0$. After solving above equation, we have

$$G_5(\zeta) = \frac{-hn_1}{1-h} + \left(w_{20}(x) + \frac{hn_1}{1-h} \right) e^{-\frac{\varepsilon(1-h)(1-\mu_1)\zeta}{a}},$$

which implies that

$$w_2(x,t) = \frac{-hn_1}{1-h} + \left(w_{20}(x) + \frac{hn_1}{1-h} \right) e^{-\frac{\varepsilon(1-h)(1-\mu_1)(x-at)}{a}}. \tag{62}$$

Now consider perturbed manifold $(\Omega_{4,\varepsilon})$ and taking $\varepsilon^2 \to 0$, we arrive at

$$-a(G_4^m)' - m[(1-\mu_1)(hG_4 + (1-h)\mu_1)]\varepsilon G_4^{m-1} = 0,$$

After solving the above equation, and the solution in x and t variables is as follows:

$$w_1(x,t) = \frac{-(1-h)\mu_1}{h} + \left(w_{10}(x) + \frac{(1-h)\mu_1}{h}\right)e^{\frac{-\varepsilon h(1-\mu_1)(x-at)}{a}}. \tag{63}$$

The perturbed manifold $(\Omega_{5,\varepsilon})$ and taking $\varepsilon^2 \to 0$, we arrive at

$$-a(G_5^m)' - m\varepsilon(1-\mu_1)(hn_2 + (1-h)G_5)G_5^{m-1} = 0,$$

which is similar to Equation (62). Therefore, the solution is as follows:

$$w_2(x,t) = \frac{-hn_2}{1-h} + \left(w_{20}(x) + \frac{hn_2}{1-h}\right)e^{\frac{-\varepsilon(1-h)(1-\mu_1)(x-at)}{a}}. \tag{64}$$

Consider perturbed manifold $(\Omega_{6,\varepsilon})$ and arrive at

$$-a(G_4^m)' - m(1-n_3)(n_3-\mu_1)(hG_4 + (1-h)n_3)G_4^{m-1} = 0,$$

After solving the above equation, and the solution in x and t variables is as follows:

$$w_1(x,t) = \frac{-(1-h)n_3}{h} + \left(w_{10}(x) + \frac{(1-h)n_3}{h}\right)e^{-\frac{h(1-n_3)(n_3-\mu_1)(x-at)}{a}}. \tag{65}$$

From the perturbed manifold $(\Omega_{7,\varepsilon})$, we have

$$-a(G_5^m)' - m\varepsilon(1-\mu_1)(hn_2 + (1-h)G_5)G_5^{m-1} = 0,$$

After solving the above equation, we get

$$w_2(x,t) = -\mu_1 + (w_{20}(x) + \mu_1)e^{\frac{-h\varepsilon(x-at)}{a}}. \tag{66}$$

6 | Numerical Methodology

The governing equation is reduced to a first-order nonlinear ordinary differential equation of the form

$$-a\frac{dG_4}{d\zeta} - m[(1-\mu_1)(hG_4 + (1-h))]G_4^{m-1} = 0, \tag{67}$$

which can be rewritten as follows:

$$\frac{dG_4}{d\zeta} = -\frac{m(1-\mu_1)}{a}\left(hG_4 + (1-h)\right)G_4^{m-1}. \tag{68}$$

The problem is solved numerically using MATLAB's built-in solver `ode45`, which is based on an explicit adaptive Runge–Kutta (4,5) method. The computation is carried out on the spatial domain $\zeta \in [0,1]$ with the initial condition

$$G_4(0) = w_{10}(0). \tag{69}$$

The solver does not use a fixed step size; instead, it employs an adaptive step-size control strategy to ensure accuracy. Unless otherwise specified, the default MATLAB tolerances are used:

$$\texttt{RelTol} = 10^{-3}, \quad \texttt{AbsTol} = 10^{-6}.$$

The numerical solution obtained from `ode45` is evaluated on a uniform grid

$$x_i = 0 + i\Delta x,\ i = 0,1,\ldots,N,\ \Delta x = \frac{1}{N},$$

using interpolation when necessary. The accuracy of the numerical solution is measured in the L^1-norm defined as follows:

$$L^1 = \sum_{i=1}^{N}|w_{\text{exact}}(x_i,t) - w_{\text{ode45}}(x_i,t)|\Delta x. \tag{70}$$

The solutions (61)–(66) show that the combustion decreases smoothly and exponentially behind or away from the moving flame front, and for large traveling-wave constant "a" then the solutions tend to initial profile. In addition, the results for the expressions (61)–(66) are depicted in Figures 1–5. From the figures, the analytical solution demonstrates that the system admits a unique, exponentially stable equilibrium solution. The numerical solution obtained using ode45 confirms the theoretical results with high accuracy. The L^1-error is shown in the Table 1. ode45 is an adaptive Runge–Kutta method of higher order. As the mesh is refined (i.e., as N increases), the numerical error reduces significantly, indicating improved accuracy and convergence of the solution.

7 | Stability of Solutions

In this section, we assume that the solutions of the system (3) are $w_{1s} + \delta w_1$ and $w_{2s} + \delta w_2$, where w_{1s} and w_{2s} are steady-state solutions, and δw_1 and δw_1 are sufficiently small perturbed solutions. The steady-state solutions for the system (3) satisfy the following equations:

$$\begin{aligned} &\frac{\partial^2 w_{1s}^m}{\partial x^2} + (1-w_{2s})(w_{2s}-\mu_1)(hw_{1s} + (1-h)w_{2s}) = 0 \\ &\frac{\partial^2 w_{2s}^m}{\partial x^2} + (1-w_{2s})(w_2-\mu_1)(hw_{1s} + (1-h)w_{2s}) = 0, \end{aligned} \tag{71}$$

where $\varepsilon = 1$. After solving the above system, we can obtain w_{1s} and w_{2s}. Now substituting $w_{1s} + \delta w_1$ and $w_{2s} + \delta w_2$ into Equation (3) and using Equation (71), we get

TABLE 1 | Comparison between exact and `ode45` solutions with L^1-error.

N	Exact solution	`ode45` solution	L^1-error
50	0.742381	0.740539	1.8421×10^{-3}
100	0.742381	0.741460	9.2114×10^{-4}
200	0.742381	0.741921	4.6038×10^{-4}
400	0.742381	0.742151	2.3011×10^{-4}
800	0.742381	0.742266	1.1502×10^{-4}
1600	0.742381	0.742323	5.7518×10^{-5}

$$\begin{aligned}\frac{\partial \delta w_1}{\partial t} &= \frac{\partial^2}{\partial x^2}(m(w_{1s})^{m-1}\delta w_1) + h(1-w_{2s})(w_{2s}-\mu_1)\delta w_1 \\ &+ [(hw_{1s}+(1-h)w_{2s})(1-2w_{2s}+\mu)+h(1-w_{2s})]\delta w_2 \\ \frac{\partial \delta w_2}{\partial t} &= \frac{\partial^2}{\partial x^2}(m(w_{2s})^{m-1}\delta w_2) + h(1-w_{2s})(w_{2s}-\mu_1)\delta w_1 \\ &+ [(hw_{1s}+(1-h)w_{2s})(1-2w_{2s}+\mu)+h(1-w_{2s})]\delta w_2,\end{aligned} \tag{72}$$

where we neglect the higher-order terms as powers of δw_1 and δw_2 as well as the product term $\delta w_1 \delta w_2$. Taking the Fourier transformation of the system (72) and considering that $\delta\widehat{w_1}(k, t)$ $\delta\widehat{w_2}(k,t)$ and are the Fourier transformations of $\delta w_1(x,t)$ and $\delta w_2(x,t)$, we get

$$\begin{aligned}\frac{d\delta\widehat{w_1}}{dt} &= -mk^2(w_{1s})^{m-1}\delta\widehat{w_1} + h(1-w_{2s})(w_{2s}-\mu_1)\delta\widehat{w_1} \\ &+ [(hw_{1s}+(1-h)w_{2s})(1-2w_{2s}+\mu)+h(1-w_{2s})]\delta\widehat{w_2}\end{aligned}, \tag{73}$$

$$\begin{aligned}\frac{d\delta\widehat{w_2}}{dt} &= -mk^2(w_{2s})^{m-1}\delta\widehat{w_2} + h(1-w_{2s})(w_{2s}-\mu_1)\delta\widehat{w_1} \\ &+ [(hw_{1s}+(1-h)w_{2s})(1-2w_{2s}+\mu)+h(1-w_{2s})]\delta\widehat{w_2}.\end{aligned} \tag{74}$$

For simplification, we assume that $A_1 = (w_{1s})^{m-1}$, $A_2 = h(1-w_{2s})(w_{2s}-\mu_1)$, $A_3 = (hw_{1s}+(1-h)w_{2s})(1-2w_{2s}+\mu)+h(1-w_{2s})$ and $A_4 = (w_{2s})^{m-1}$, therefore, the Equations (73) and (74) become

$$\frac{d\delta\widehat{w_1}}{dt} = (-mA_1k^2 + A_2)\delta\widehat{w_1} + A_3\delta\widehat{w_2}\ , \tag{75}$$

$$\frac{d\delta\widehat{w_2}}{dt} = A_2\delta\widehat{w_1} + (-mA_4k^2 + A_2)\delta\widehat{w_2}. \tag{76}$$

The matrix form of Equations (73) and (74) is given as follows:

$$\frac{d}{dt}\begin{pmatrix}\delta\widehat{w_1} \\ \delta\widehat{w_2}\end{pmatrix} = \begin{pmatrix}-mA_1k^2 + A_2 & A_3 \\ A_2 & -mA_4k^2 + A_3\end{pmatrix}\begin{pmatrix}\delta\widehat{w_1} \\ \delta\widehat{w_2}\end{pmatrix}, \tag{77}$$

The characteristic equation is of the form

$$\det\begin{pmatrix}-mA_1k^2 + A_2 - \lambda & A_3 \\ A_2 & -mA_4k^2 + A_3 - \lambda\end{pmatrix} = 0, \tag{78}$$

which implies that

$$\begin{aligned}&\lambda^2 + \lambda(mA_1k^2 + mA_4k^2 - A_2 - A_3) \\ &+ m^2A_1A_4k^4 - mA_1A_3k^2 - mA_2A_4k^2 = 0.\end{aligned} \tag{79}$$

After solving, the eigenvalues λ_1 and λ_2 are given as follows:

$$\begin{aligned}\lambda_1 &= \frac{1}{2}[-(mA_1k^2 + mA_4k^2 - A_2 - A_3) \\ &- \sqrt{(mA_1k^2 + mA_2k^2 - A_2 - A_3)^2 - 4(m^2A_1A_4k^4 - mA_1A_3k^2 - mA_2A_4k^2)}\,],\end{aligned} \tag{80}$$

and

$$\begin{aligned}\lambda_2 &= \frac{1}{2}[-(mA_1k^2 + mA_4k^2 - A_2 - A_3) \\ &+ \sqrt{(mA_1k^2 + mA_4k^2 - A_2 - A_3)^2 - 4(m^2A_1A_4k^4 - mA_1A_3k^2 - mA_2A_4k^2)}\,].\end{aligned} \tag{81}$$

The eigenvectors corresponding to the eigenvalues are as follows:

$$\left\{\frac{-mA_1k^2 + mA_4k^2 - A_2 + A_3 - A_5}{2A_2}, 1\right\}, \tag{82}$$

and

$$\left\{\frac{-mA_1k^2 + mA_4k^2 - A_2 + A_3 + A_5}{2A_2}, 1\right\}, \tag{83}$$

where

$$A_5 = \sqrt{(mA_1k^2 + mA_4k^2 - A_2 - A_3)^2 - 4(m^2A_1A_4k^4 - mA_1A_3k^2 - mA_2A_4k^2)}. \tag{84}$$

After finding the eigenvalues and eigenvectors, we can write the general solution as follows:

$$\begin{aligned}\begin{pmatrix}\delta\widehat{w_1}(k,t) \\ \delta\widehat{w_2}(k,t)\end{pmatrix} &= A_6e^{\lambda_1 t}\begin{pmatrix}\frac{-mA_1k^2 + mA_4k^2 - A_2 + A_3 - A_5}{2A_2} \\ 1\end{pmatrix} \\ &+ A_7e^{\lambda_2 t}\begin{pmatrix}\frac{-mA_1k^2 + mA_4k^2 - A_2 + A_3 + A_5}{2A_2} \\ 1\end{pmatrix},\end{aligned} \tag{85}$$

where A_6 and A_7 can be obtained by using the initial conditions. Since $\delta\widehat{w_1}(k,0) = \delta\widehat{w}_{10}(k)$ and $\delta\widehat{w}_2(k,0) = \delta\widehat{w}_{20}(k)$, the following assessment hold:

$$\begin{aligned}\begin{pmatrix}\delta\widehat{w}_{10}(k) \\ \delta\widehat{w}_{20}(k)\end{pmatrix} &= A_6\begin{pmatrix}\frac{-mA_1k^2 + mA_4k^2 - A_2 + A_3 - A_5}{2A_2} \\ 1\end{pmatrix} \\ &+ A_7\begin{pmatrix}\frac{-mA_1k^2 + mA_4k^2 - A_2 + A_3 + A_5}{2A_2} \\ 1\end{pmatrix},\end{aligned} \tag{86}$$

which implies that

$$\begin{aligned} &A_6(-mA_1k^2 + mA_4k^2 - A_2 + A_3 - A_5) \\ &+ A_7(-mA_1k^2 + mA_4k^2 - A_2 + A_3 + A_5) = 2A_2\delta\widehat{w}_{10}(k), \end{aligned} \tag{87}$$

and

$$A_6 + A_7 = \delta\widehat{w}_{20}(k). \tag{88}$$

After solving Equations (87) and (88), we get

$$A_6 = -\frac{2A_2\delta\widehat{w}_{10}(k) + (-mA_1k^2 + mA_4k^2 - A_2 + A_3 - 3A_5)\delta\widehat{w}_{20}(k)}{2A_5}, \tag{89}$$

and

$$A_7 = \frac{2A_2\delta\widehat{w}_{10}(k) - (-mA_1k^2 + mA_4k^2 - A_2 + A_3 - A_5)\delta\widehat{w}_{20}(k)}{2A_5}. \tag{90}$$

From Equation (85), we have

$$\begin{aligned} \delta\widehat{w_1}(k,t) \;=\; &A_6\left(\frac{-mA_1k^2 + mA_4k^2 - A_2 + A_3 - A_5}{2A_2}\right)e^{\lambda_1 t} \\ &+ A_7\left(\frac{-mA_1k^2 + mA_4k^2 - A_2 + A_3 + A_5}{2A_2}\right)e^{\lambda_2 t}, \end{aligned} \tag{91}$$

and

$$\delta\widehat{w_2}(k,t) = A_6e^{\lambda_1 t} + A_7e^{\lambda_2 t}. \tag{92}$$

Now, for the solutions in the original physical variables (x,t), we shall apply the inverse Fourier transformation on Equations (90) and (91) to get

$$\begin{aligned} \delta w_1(k,t) \;=\; &\frac{1}{2\pi}\int_R A_6\left(\frac{-mA_1k^2 + mA_4k^2 - A_2 + A_3 - A_5}{2A_2}\right)e^{\lambda_1 t + ikx}dk \\ &+ \frac{1}{2\pi}\int_R A_7\left(\frac{-mA_1k^2 + mA_4k^2 - A_2 + A_3 + A_5}{2A_2}\right)e^{\lambda_2 t + ikx}dk, \end{aligned} \tag{93}$$

and

$$\delta w_2(k,t) = \frac{1}{2\pi}\int_R (A_6e^{\lambda_1 t} + A_7e^{\lambda_2 t})e^{ikx}dk, \tag{94}$$

where $A_1 = (w_{1s})^{m-1}$, $A_2 = h(1-w_{2s})(w_{2s}-\mu_1)$, $A_3 = (hw_{1s} + (1-h)w_{2s})(1-2w_{2s}+\mu) + h(1-w_{2s})$, $A_4 = (w_{2s})^{m-1}$, λ_1, λ_2, A_5, A_6, and A_7 are given in Equations (80), (81), (84), (89) and (90) respectively.

For the stability of the system, we consider the eigenvalues which are given by Equations (80) and (81). If λ_1 and λ_2 are real eigenvalues then

$$\begin{aligned} \Delta = &(mA_1k^2 + mA_4k^2 - A_2 - A_3)^2 \\ &- 4(m^2A_1A_4k^4 - mA_1A_3k^2 - mA_2A_4k^2) > 0, \end{aligned}$$

and the system is stable if $mA_1k^2 + mA_4k^2 - A_2 - A_3 > 0$ and $m^2A_1A_4k^4 - mA_1A_3k^2 - mA_2A_4k^2 > 0$. If λ_1 and λ_2 are complex eigenvalues then $\Delta < 0$ and the system is sable if $mA_1k^2 + mA_4k^2 - A_2 - A_3 > 0$.

8 | Short-Time Asymptotic Expansion

We consider now the behavior of solutions $w_1(x,t)$ and $w_2(x,t)$ for small times for which we employ matched asymptotic expansions and integral transform techniques. These methods will help to analytically obtain the solution in both the inner (near the initial condition) and outer (large-scale) regions. The goal is to capture the flame front's behavior during the early stages of the process.

At small times, the behavior near the initial condition typically forms an initial layer. We seek an expansion in powers of t^α, where α is a parameter to be determined from the scaling analysis. Let us propose the following expansions:

$$w_1(x,t) = w_{1_0}(x) + t^\alpha w_{1_1}(x) + t^{2\alpha}w_{1_2}(x) + \cdots,$$

$$w_2(x,t) = w_{2_0}(x) + t^\alpha w_{2_1}(x) + t^{2\alpha}w_{2_2}(x) + \cdots.$$

To determine the correct scaling of t, we perform a balance of terms in the governing Equation (3). The diffusion terms contain second-order spatial derivatives and must balance with the reaction terms for small times. We begin by considering the dominant terms in both diffusion and reaction components:

$$\frac{\partial^2 w_1^m}{\partial x^2} \sim t^\alpha \text{ and } G(w_1, w_2) \sim t^\alpha.$$

The reaction term $G(w_1, w_2)$ behaves linearly for short times. Assuming an initial condition that is spatially smooth, the second derivative term scales as t^α. Therefore, we balance diffusion and reaction terms and choose $\alpha = 1$, leading to:

$$w_1(x,t) = w_{1_0}(x) + t w_{1_1}(x) + t^2 w_{1_2}(x) + \cdots,$$

$$w_2(x,t) = w_{2_0}(x) + t w_{2_1}(x) + t^2 w_{2_2}(x) + \cdots.$$

Substituting these expansions into the original equations and collecting terms of order t^0, we recover the initial condition $w_1(x,0) = w_{1_0}(x),\ w_2(x,0) = w_{2_0}(x)$. The first-order terms can be obtained based on a Fourier transformation. We substitute into the PDE system and obtain the following linear PDEs for $w_{1_1}(x)$ and $w_{2_1}(x)$:

$$w_{1_1} = \frac{\partial^2 \left(w_{1_0}^m\right)}{\partial x^2} + \left(1 - w_{2_0}\right)\left(w_{2_0} - \mu_1\right) w_{3_0}, \tag{95}$$

$$w_{2_1} = \varepsilon \frac{\partial^2 \left(w_{2_0}^m\right)}{\partial x^2} + \left(1 - w_{2_0}\right)\left(w_{2_0} - \mu_1\right) w_{3_0}, \tag{96}$$

where $w_{3_0} = h w_{1_0} + (1-h) w_{2_0}$. Now, the Fourier transform of the first equation is as follows:

$$\widehat{w}_{1_1}(k) = -k^2 \mathscr{F}\left(w_{1_0}^m\right) + \mathscr{F}\left(\left(1 - w_{2_0}\right)\left(w_{2_0} - \mu_1\right) w_{3_0}\right). \tag{97}$$

Similarly, for the second equation, the Fourier transform becomes:

$$\widehat{w}_{2_1}(k) = -\varepsilon k^2 \mathscr{F}\left(w_{2_0}^m\right) + \mathscr{F}\left(\left(1 - w_{2_0}\right)\left(w_{2_0} - \mu_1\right) w_{3_0}\right). \tag{98}$$

After operating with particular initial data $w_{1_0}(x), w_{2_0}(x)$, and making the inverse Fourier transformation, we can recover the original physical spatial variable.

Now, for large x or large t, we employ an outer expansion. Let $w_1(x,t)$ and $w_2(x,t)$ admit the expansions:

$$w_1(x,t) = W_{1_0}(x,t) + t^\beta W_{1_1}(x,t) + \cdots,$$

$$w_2(x,t) = W_{2_0}(x,t) + t^\beta W_{2_1}(x,t) + \cdots,$$

where β is to be determined based on a scaling argument.

Now, using matched asymptotic expansions, we match the inner and outer expansions in an intermediate regime. This ensures a smooth transition between the small-time and large-time behavior of the solution. The matching condition is imposed by ensuring that the leading-order terms in the inner and outer expansions agree asymptotically as $x \to \infty$ or $t \to 0$. We are particularly interested in the behavior of the inner expansion in the limit as $x \to \infty$ for each fixed t (i.e., far from the flame front). The goal is to find the asymptotic behavior of the inner expansion as $x \to \infty$.

We assume that for large x, the solution behaves like:

$$w_1(x,t) \sim A_1 + \frac{B_1(t)}{x^\alpha} + \cdots, \quad x \to \infty, \tag{99}$$

$$w_2(x,t) \sim A_2 + \frac{B_2(t)}{x^\beta} + \cdots, \quad x \to \infty, \tag{100}$$

where A_1, A_2 are constants, and $B_1(t), B_2(t)$ are functions of time. The exponents α and β are determined by solving the leading-order behavior of the governing equations as $x \to \infty$.

The outer expansion describes the solution for large x or large t, where the diffusion effects dominate over the reaction terms. We assume that the outer solution takes the form of a series expansion in powers of t^γ, where γ is to be determined:

$$W_1(x,t) = W_{1_0}(x,t) + t^\gamma W_{1_1}(x,t) + t^{2\gamma} W_{1_2}(x,t) + \ldots,$$

$$W_2(x,t) = W_{2_0}(x,t) + t^\gamma W_{2_1}(x,t) + t^{2\gamma} W_{2_2}(x,t) + \ldots.$$

For large x, the diffusion terms become dominant, so we expect the outer solution to satisfy a simpler, linearized version of the original system. Assuming that the dominant behavior in this regime is diffusive, we focus on the leading-order terms of the system.

In the outer region (for large x and t), the behavior of the solution must match the inner solution as $x \to 0$ (or $t \to 0$). Therefore, we look for the asymptotic behavior of the outer solution as $x \to 0$. Typically, we assume that

$$W_1(x,t) \sim C_1 + t x^\delta + \cdots, \quad x \to 0, \tag{101}$$

$$W_2(x,t) \sim C_2 + t x^\eta + \cdots, \quad x \to 0, \tag{102}$$

where C_1, C_2 are constants, and δ, η are determined by solving the outer equations in the small-x limit.

Now, we make use of Van Dyke's matching principle, which states that the inner expansion as $x \to \infty$ must match the outer expansion as $x \to 0$. Specifically, the terms in the inner expansion in powers of x must match those in the outer expansion as $x \to 0$.

From the inner expansion, we have the asymptotic behavior as $x \to \infty$ given in expressions (99) and (100). From the outer expansion, we have the asymptotic behavior as $x \to 0$, given in expressions (101) and (102). We impose matching conditions by equating the asymptotic behaviors of the inner and outer expansions. This gives the following conditions:

1. The constant terms must match:

$$A_1 = C_1,\ A_2 = C_2.$$

2. The powers of x must match, giving the relationships between the exponents. We hence require the following exponent:

$$\alpha = -\delta,$$

and this value will fix a relation between β and η as it will be further described.

3. The coefficients of the next-order terms must also match:

$$B_1(t) = t,\ B_2(t) = t.$$

To refine the matching, we solve for the exponents $\alpha, \beta, \delta, \eta$ by performing a scaling analysis of the governing equations. This involves balancing the dominant terms in the PDEs as $x \to \infty$ (for the inner solution) and as $x \to 0$ (for the outer solution).

We start by considering the leading-order diffusion terms in the inner expansion:

$$\frac{\partial^2 w_1}{\partial x^2} \sim \frac{B_1(t)}{x^{\alpha+2}}.$$

Balancing this term with the reaction terms gives a relationship for α. Similarly, for the outer solution, we balance the diffusion terms with the reaction terms as $x \to 0$:

$$\frac{\partial^2 W_1}{\partial x^2} \sim \frac{t}{x^{2-\delta}}.$$

For the inner expansion, the leading-order diffusion term for $w_1(x,t)$ in the governing PDE is given by $\frac{\partial^2 w_1^m}{\partial x^2}$, then

$$\frac{\partial^2 w_1^m}{\partial x^2} \sim \frac{\partial^2}{\partial x^2}\left(A_1^m + \frac{B_1(t)^m}{x^{\alpha m}}\right).$$

Since the constant A_1^m term vanishes after differentiation, we focus on the second term:

$$\frac{\partial^2 w_1^m}{\partial x^2} \sim \frac{\partial^2}{\partial x^2}\left(\frac{B_1(t)^m}{x^{\alpha m}}\right) = \frac{B_1(t)^m}{x^{\alpha m+2}}(\alpha m)(\alpha m+1).$$

Thus, the diffusion term scales as follows:

$$\frac{\partial^2 w_1^m}{\partial x^2} \sim \frac{B_1(t)^m \alpha m(\alpha m+1)}{x^{\alpha m+2}}.$$

Now, let us analyze the reaction term $G(w_1, w_2)$. For large x, $G(w_1, w_2)$ behaves as follows:

$$G(w_1, w_2) \sim (1 - w_2)(w_2 - \mu_1)w_3.$$

Assuming $w_2(x,t) \sim A_2 + \frac{B_2(t)}{x^\beta}$, we have:

$$w_3 = hw_1 + (1-h)w_2 \sim hA_1 + (1-h)A_2 + \frac{hB_1(t)}{x^\alpha} + \frac{(1-h)B_2(t)}{x^\beta}.$$

Thus, the reaction term scales as follows:

$$G(w_1, w_2) \sim \left(1 - A_2 - \frac{B_2(t)}{x^\beta}\right)\left(A_2 - \mu_1 + \frac{B_2(t)}{x^\beta}\right)$$
$$\left(hA_1 + (1-h)A_2 + \frac{hB_1(t)}{x^\alpha} + \frac{(1-h)B_2(t)}{x^\beta}\right).$$

We consider that the reaction term scales as follows:

$$G(w_1, w_2) \sim \frac{C_1(t)}{x^{\beta+\alpha}},$$

where $C_1(t)$ is a function of time that depends on the constants $A_1, A_2, B_1(t), B_2(t)$. In the inner region, we balance the diffusion term $\frac{1}{x^{\alpha m+2}}$ with the reaction term $\frac{1}{x^{\beta+\alpha}}$ to obtain a relationship between α and β. Thus, we require:

$$\alpha m + 2 = \beta + \alpha, \quad \alpha = \frac{\beta - 2}{m - 1}.$$

This provides the first relation between the exponents α and β. Now, consider the outer expansion for large x in Equation (101). In the outer region, the dominant diffusion term for $W_1(x,t)$ behaves similarly, and we assume the form:

$$W_1(x,t) \sim C_1 + tx^\delta + \cdots,\ x \to 0.$$

The second derivative of W_1^m with respect to x is as follows:

$$\frac{\partial^2 W_1^m}{\partial x^2} \sim \frac{\partial^2}{\partial x^2}(C_1^m + t^m x^{\delta m}) = t^m \frac{\partial^2}{\partial x^2}(x^{\delta m}) = t^m \delta m(\delta m - 1)x^{\delta m - 2}.$$

Thus, the diffusion term scales as follows:

$$\frac{\partial^2 W_1^m}{\partial x^2} \sim \frac{t^m}{x^{2-\delta m}}.$$

The reaction term $G(W_1, W_2)$ in the outer region scales similarly to:

$$G(W_1, W_2) \sim \frac{C_2(t)}{x^{\eta+\delta}},$$

where η is another exponent in Equation (102). Hence, the following relation holds after balancing the diffusion and reaction terms in the outer regime:

$$2 - \delta m = \eta + \delta, \quad \delta = \frac{2 - \eta}{m + 1}.$$

Using Van Dyke's matching principle, the exponents from the inner and outer expansions must satisfy:

$$\alpha = -\delta.$$

Thus, we have the following relation between β and η:

$$\frac{\beta - 2}{m + 1} = \frac{\eta - 2}{m + 1},$$

leading to $\beta = \eta$. From the matched-asymptotic derivation η is not an exact value. The best value satisfies $\eta \geq 0$. If $\eta < 0$ then the curvature blows up, infinite diffusion flux and is physically unacceptable. So we assume $\eta = 2$ because the diffusion controlled outer region and ensures a smooth physical transition in the outer region when $x \to 0$, as expressed in Equation (102). Then, we obtain $\delta = 0$, which suggests that the outer solution grows as $x \to 0$, indicating that the flame front has a highly localized behavior. Under this approach, the combustion is extremely rapid near the flame front, leading to a rapid change in the flame pressure and temperature variables over a small region. Furthermore, we recall that the diffusion term for W_2 and the reaction term $G(W_1, W_2)$ scale differently. Selecting $\eta = 2$ allows the exponents of these terms to satisfy the scaling relationship necessary for the dominant balance between diffusion and reaction, ensuring that neither term overwhelms the other. As a consequence of the selected value of η, we have that $\beta = 2$ and $\alpha = 0$. We have then connected the inner (short-time) solution with the outer (large-time or large-distance) solution for the flame propagation model. By applying Van Dyke's matching principle, we ensure that the asymptotic behavior of the solutions is consistent in both regimes.

9 | Conclusion

In this study, we developed a mathematical model to describe flame propagation influenced by temperature and pressure using the framework of nonlinear diffusion and porous structure theory. The model is analyzed through several analytical techniques, each contributing to a deeper understanding of flame dynamics. First, the Hopf bifurcation analysis identified the equilibrium points where the system's solutions are asymptotically stable. This provides a foundation for predicting the long-term behavior of the flame under varying conditions. Second, we derived the solution profiles using the traveling wave approach and geometric perturbation theory. These approaches allow us to capture the behavior of the flame as it propagates through space and time. Third, we demonstrated the existence of a finite speed of propagation for the flame, ensuring that the model adheres to realistic physical constraints. Fourth, we developed the numerical solution for perturbing the problem to validate our results. Finally, by employing the method of matched asymptotic expansions, we connected the short-time (inner) and large-time or large-distance (outer) solutions. Through Van Dyke's matching principle, we ensured consistency between these regimes, providing a comprehensive view of the flame's behavior across different time scales.

Overall, this work provided an analytical framework for understanding flame dynamics in a nonlinear diffusion context, taking into account both short- and long-term behaviors. The conditions for stability and propagation speed introduced practical information into flame control and prediction. In future work, one can extend this model to fourth-order partial differential equations.

Figure 6 shows that for $T_n < 0$ and $D_n > 0$, it follows that the real parts of the eigenvalues remain negative for all admissible values of n_3, which ensures the stability of the system.

Figure 7 shows that for the particular values of $T_n > 0$ and $D_n > 0$ for $n = 1$ with $n_1 \geq 0$. The sum and product of the roots are given by $-(T_n)$ and D_n, respectively. Hence, both eigenvalues possess negative real parts. This implies that the system is asymptotically stable for all admissible values of n_1.

Figure 8 shows that for the particular case $T_n < 0$ and $D_n > 0$ for $n = 1$, and taking

$$n_2 \leq \mu_1 - \frac{\mu_1}{h} + \frac{n^{2m}\mu_1^m}{hl^2(1-\mu_1)},$$

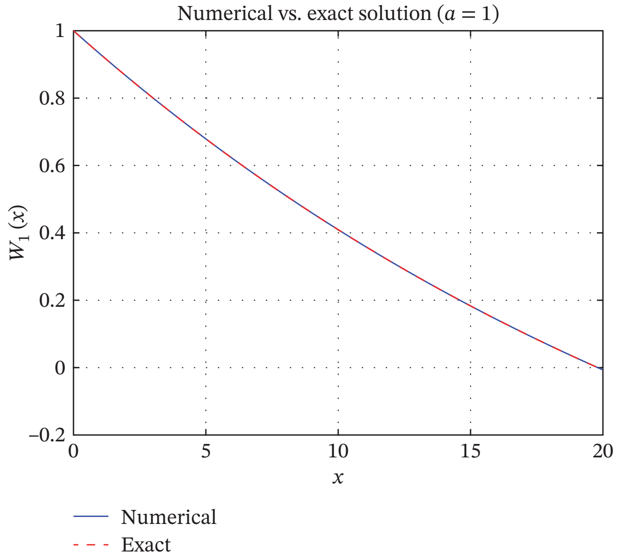

FIGURE 1 | Representation of solutions of Equation (61) for the case $t = 1$, $\varepsilon = 0.1$, $h = 0.5$, $\mu_1 = 0.3$, $w_{10} = 100$, and $a = 1$.

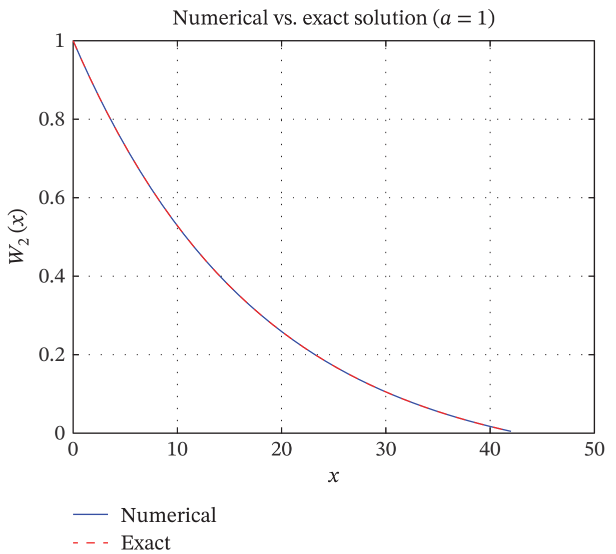

FIGURE 2 | Representation of solutions of Equation (62) for the case $t = 1$, $\varepsilon = 0.1$, $h = 0.5$, $\mu_1 = 0.3$, $n_1 = 0.4$, $w_{20} = 100$, and $a = 1$.

then, the real parts of both eigenvalues remain negative, ensuring the asymptotic stability of the system.

Figures 1–5 show that the analytical and numerical solutions of Section 5 are identical. The graph represents that the traveling wave solutions for flame propagation in which the temperatures $w_1(x)$ and $w_2(x)$ decrease from a high value to a low value as x increases.

Figure 9 represents the variation of real parts of eigenvalues, which are the function of k. The graph shows that for all values k, the eigenvalues are negative and decrease exponentially.

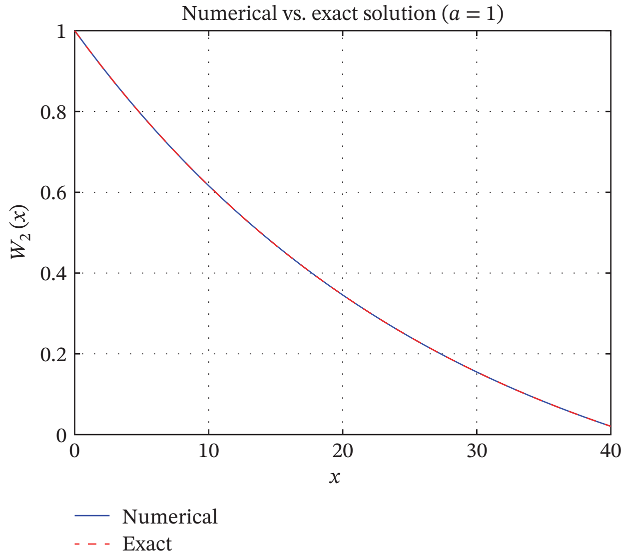

FIGURE 3 | Representation of solutions of Equation (63) for the case $t=1$, $\varepsilon=0.1$, $h=0.5$, $\mu_1=0.3$, $w_{10}=100$, and $a=1$.

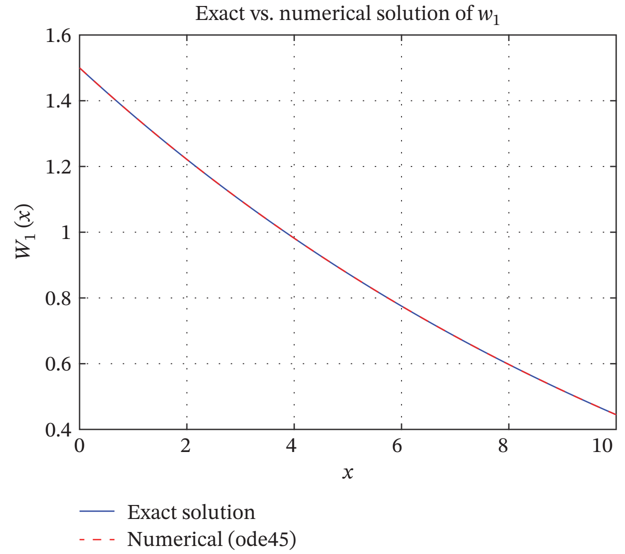

FIGURE 5 | Representation of solutions of Equation (66) for the case $t=1$, $\varepsilon=0.1$, $h=0.5$, $\mu_1=0.3$, $w_{20}=100$, and $a=1$.

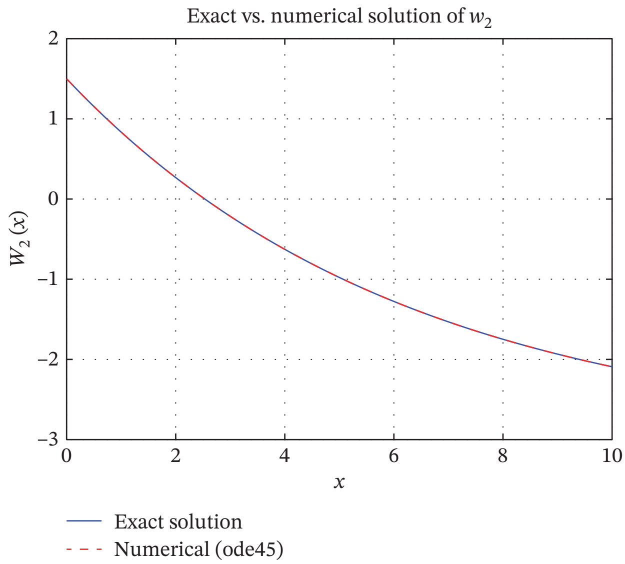

FIGURE 4 | Representation of solutions of Equation (65) for the case $t=1$, $n_3=0.5$, $\varepsilon=0.1$, $h=0.5$, $\mu_1=0.3$, $w_{10}=100$, and $a=1$.

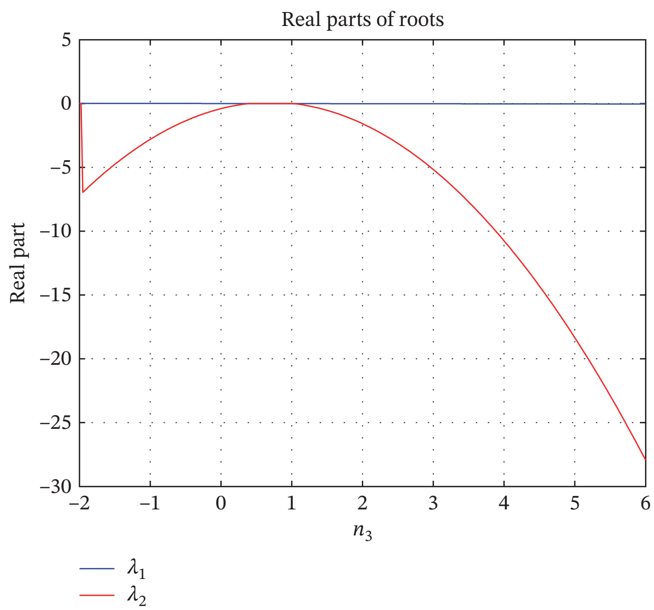

FIGURE 6 | Representation of solutions of Equation (7) for the case $m=2$, $l=25$, $n=1$, $h=0.3$, and $\mu_1=0.4$.

Further if k increases, then the eigenvalues become more negative, which shows that as the diffusion effects increase, the high frequency perturbation (or short wavelength) rapidly decays. Also near to $k=0$, the eigenvalues are still negative but closed to zero, which indicates the long-wavelength perturbations decay slowly. So, the solution is stable.

Figures 10 and 11 represent the spatial profile of the perturbations δw_1 and δw_2 at time $t=10$. It is shown that in most of the domain δw_1 and δw_2 are zero, and close to the boundaries of δw_1 the small negative deviation appears while close to the boundaries of δw_2 the small positive deviation appears, which shows that the imposed disturbance does not have much effect. This indicates that the solution is stable under a small disturbance.

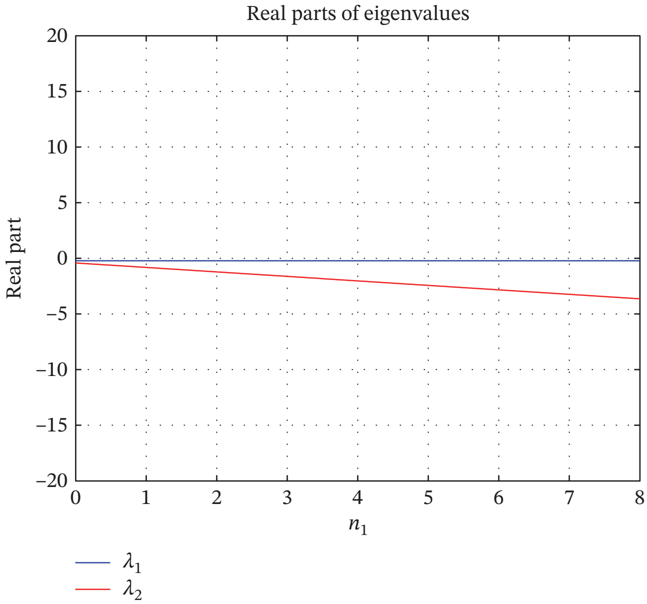

FIGURE 7 | Representation of solutions of Equation (13) for the case $m = 2$, $l = 3$, $n = 1$, $h = 0.3$, and $\mu_1 = 0.4$.

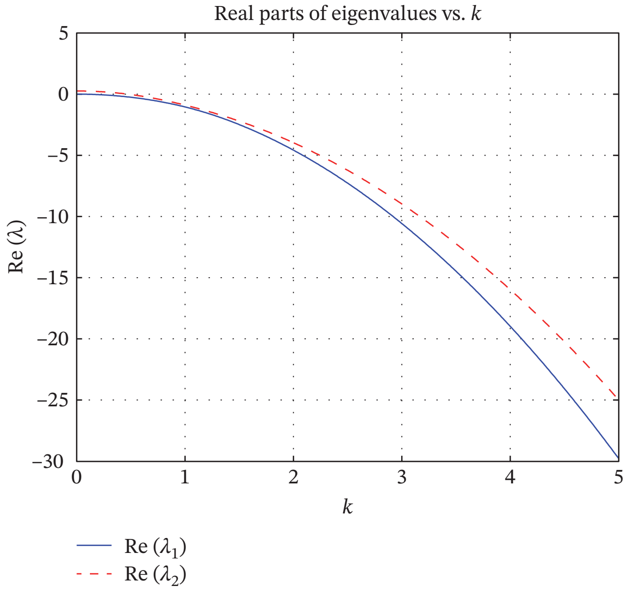

FIGURE 9 | Representation of solutions of Equations (80) and (81) for the case $m = 2$, $h = 0.3$, $\mu_1 = 0.4$, $w_{1s} = 0.5$, and $w_{2s} = 0.6$.

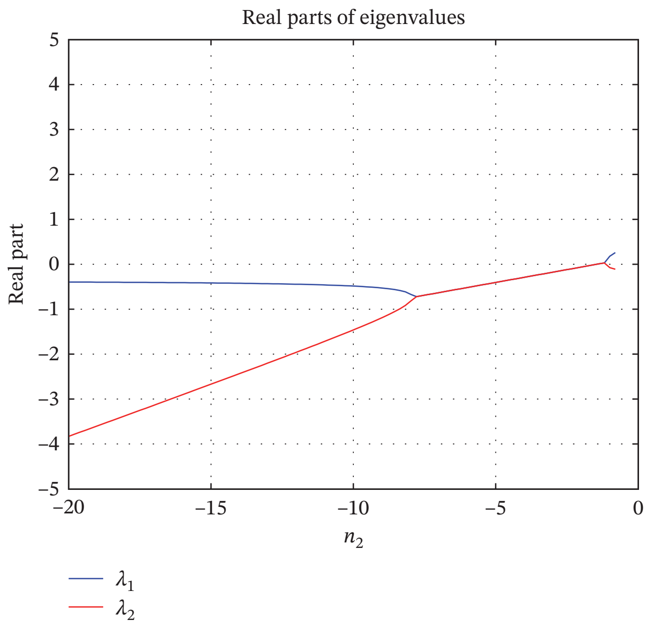

FIGURE 8 | Representation of solutions of Equation (20) for the case $m = 2$, $l = 3$, $n = 1$, $h = 0.3$, and $\mu_1 = 0.4$.

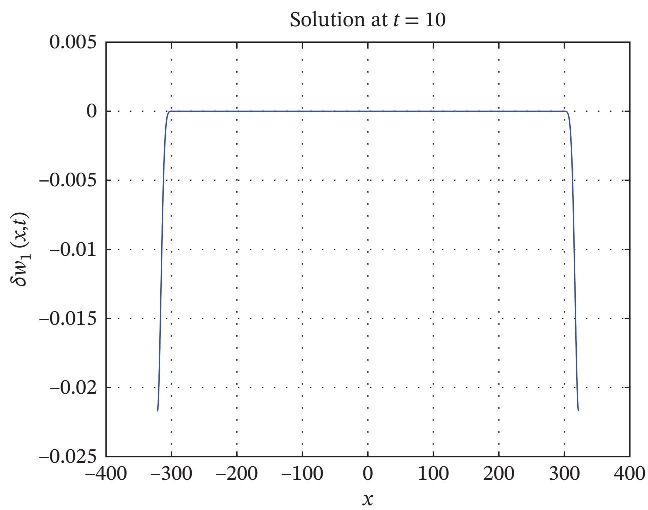

FIGURE 10 | Representation of solutions of Equation (93) for the case $t = 10$. $m = 2$, $h = 0.3$, $\mu_1 = 0.4$, $k = 1$, $w_{1s} = 0.9 w_{2s} = 0.9$, $\delta\widehat{w}_{10} = 0.05$, and $\delta\widehat{w}_{20} = 0.06$.

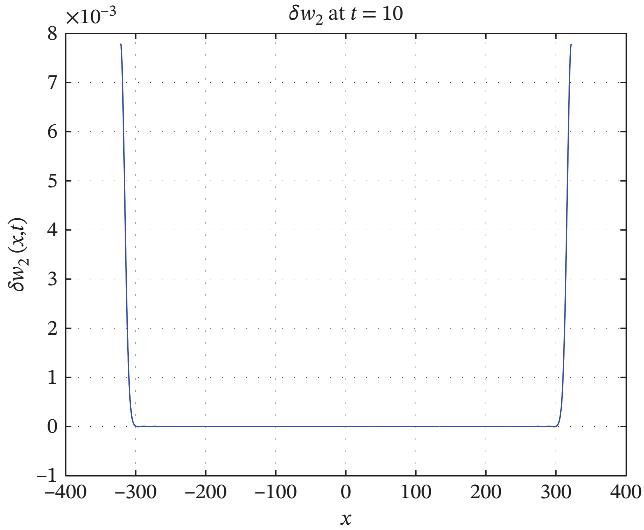

FIGURE 11 | Representation of solutions of Equation (94) for the case $t = 10$, $m = 2$, $h = 0.3$, $\mu_1 = 0.4$, $k = 1$, $w_{1s} = 0.9 w_{2s} = 0.9$, $\delta\widehat{w}_{10} = 0.05$, and $\delta\widehat{w}_{20} = 0.06$.

Author Contributions

Saqib Zia: supervision, formal analysis. **Saeed ur Rahman**: methodology and formal analysis. **José Luis Díaz Palencia**: writing – original draft. **Ghania Zia**: MATLAB software use to obtain the figures. **Wei Sin Koh**: validation. **Sultan Hussain**: numerical simulation.

Acknowledgments

This work was supported and funded by the Deanship of Scientific Research at Imam Mohammad Ibn Saud Islamic University (IMSIU) (Grant IMSIU-DDRSP2603).

Funding

No funding was received for this research.

Disclosure

All authors read, approved, and agreed to the published final version of the manuscript. The authors declare that the preprint of this article is already published (Rahman et. al [29]).

Conflicts of Interest

The authors declare no conflicts of interest.

Data Availability Statement

Data sharing is not applicable to this article as no datasets were generated or analyzed during the current study.

References

1. IPCC, "Climate Change, Synthesis Report," IPCC Plenary XXVII (2007).

2. M. M. Kamal and A. A. Mohamad, "Combustion in Porous Media," *Proceedings of the Institution of Mechanical Engineers Part A: Journal of Power and Energy* 220, no. 5: 487–508.

3. B. M. Ali, M. B. Riaz, N. S. S. Singh, W. Abdelfattah, and M. Jawad, "Bioconvective MHD Flow of Willaimson Nanofluid With Swimming Microorganisms and Cross-Diffusion Effects Induced by Nonlinear Stretching Surface in Porous Media," *Results in Engineering* 27 (2025): 105660.

4. P. Gordon, "Quenching and Propagation of Combustion Fronts in Porous Media," *Communications in Mathematical Sciences* 4, no. 2 (2006): 471–479.

5. R. A. Fisher, "The Wave of Advance of Advantageous Genes," *Annals of Eugenics* 7, no. 4 (1937): 355–369.

6. J. Billingham and D. J. Needham, "The Development of Travelling Waves in Quadratic and Cubic Autocatalysis With Unequal Diffusion Rates. II. An Initial-Value Problem With an Immobilized or Nearly Immobilized Autocatalyst," *Philosophical Transactions of the Royal Society of London. Series A: Physical and Engineering Sciences* 1644 (1991): 497–539.

7. A. N. Kolmogorov, I. G. Perrovsky, and N. S. Piskunov, "A Study of the Equation of Diffusion With Increase in the Quantity of Matter and Its Application to a Biological Problem," *Journal Bulletin of Moscow University* 1 (1937): 1–26.

8. H. F. Weinberger, "On Spreading Speeds and Traveling Waves for Growth and Migration Models in a Periodic Habitat," *Journal of Mathematical Biology* 45, no. 6 (2002): 511–548.

9. K. I. Schelkin, "Influence of the Tube Walls Roughness on the Onset and Propagation of Detonation in Gases Sov," *Journal of Experimental and Theoretical Physics* 10 (1940): 823–827.

10. I. Brailovsky, V. Goldshtein, I. Shreiber, and G. Sivashinsky, "On Combustion Waves Driven by Diffusion of Pressure," *Combustion Science and Technology* 124, no. 1–6 (2007): 145–165.

11. P. Gordon, "Recent Mathematical Results on Combustion in Hydraulically Resistant Porous Media," *Mathematical Modelling of Natural Phenomena* 2, no. 2 (2007): 56–76.

12. A. Ghazaryan and P. Gordon, "KPP Type Flame Fronts in Porous Media," *Nonlinearity* 21, no. 5 (2008): 973–992.

13. D. G. Aronson and H. F. Weinberger, "Nonlinear Diffusion in Population Genetics, Combustion, and Nerve Pulse Propagation," in *Partial Differential Equations and Related Topics*, (Springer, 2006): 5–49.

14. Y. I. Kanel, "On the Stability of Solutions of the Cauchy Problem for Equations Arising in the Theory of Combustion," *Materials* 59 (1962): 245–288.

15. V. Roussier, "Stability of Radially Symmetric Travelling Waves in Reaction-Diffusion Equations," *Annales de l'Institut Henri Poincaré C, Analyse Non Linéaire* 21, no. 3 (2004): 341–379.

16. S. U. Rahman and J. L. D. Palencia, "Analytical and Computational Approaches for Bi-Stable Reaction and p-Laplacian Diffusion Flame Dynamics in Porous Media," *Mathematics* 12 (2024): 216.

17. M. Chen, Z. Hu, Q. Zheng, and H. M. Srivastava, "Dynamics Analysis of a Spatiotemporal SI Model," *Alexandria Engineering Journal* 74 (2023): 705–714.

18. M. Chen, Z. Ling, and C. Tian, "Dynamics of a Zooplankton-Phytoplankton Model Incorporating Phytoplankton-Taxis," *Discrete and Continuous Dynamical Systems - B* 33 (2026): 1–34.

19. Kiselev, *Fundamentals of Diffusion MRI (Magnetic Resonance Imaging) Physics* (Wiley Online Library, 2017).

20. E. F. Keller and L. A. Segel, "Traveling Bands of Chemotactic Bacteria: A Theoretical Analysis," *Journal of Theoretical Biology* 30, no. 2 (1971): 235–248.

21. R. Ellahi, F. Hussain, and F. Ishtiaq, "Peristaltic Transport of Jeffrey Fluid in a Rectangular Duct Through a Porous Medium Under the Effect of Partial Slip: An Application to Upgrade Industrial Sieves/Filters," *Pramana* 93 (2019): 34.

22. J. D. Palencia, "Analytical Assessments to Model a Flame Propagation With a Porous Medium Equation," *Computational and Applied Mathematics* 41 (2022): 164.

23. G. Guo, B. Guo, M. Wei, and J. Wu, “Hopf Bifurcation and Steady-State Bifurcation for an Autocatalysis Reaction-Diffusion Model,” *Journal of Mathematical Analysis and Applications* 391 (2012): 265–277.

24. M. Chen and R. Wu, “Dynamics of a Harvested Predator–Prey Model With Predator-Taxis,” *Bulletin of the Malaysian Mathematical Sciences Society* 46, no. 2 (2023): 76.

25. M. Chen and H. Srivastava, “Existence and Stability of Bifurcating Solution of a Chemotaxis Model,” *Proceedings of the American Mathematical Society* 151, no. 11 (2023): 4735–4749.

26. M. Chen, C. Tian, S. Ham, H. Kim, and J. Kim, “Impact of Prey-Taxis on a Harvested Intraguild Predation Predator-Prey Model,” *European Journal of Applied Mathematics 36* 6 (2025): 1183–1220.

27. M. Chen, X.-Z. Li, and C. Tian, “Determining Turing Instability of the Periodic Solution of a Predator–Prey Model,” *Applied Mathematics Letters* 171 (2025): 109689.

28. M. Chen, X. Li, X. Z. Li, and R. Wu, “Turing Instability of Equilibrium and Periodic Solution for an Enzyme-Catalyzed System,” *MATCH Communications in Mathematical and in Computer Chemistry* 95, no. 1 (2026): 659–694.

29. S. Rahman, J. L. Palencia, and G. Zia, “Hopf Bifurcation Analysis and Matched Asymptotics for a Bi-Stable Flame Propagation Model,” Available SSRN.